MAGNETOHYDRODYNAMICS Vol. 57 (2021), No. 1, pp. 73–84
DOI: 10.22364/mhd.57.1.6

MODEL OF ELECTROMAGNETIC PURIFICATION OF LIQUID METAL

G. Losev, A. Mamykin, I. Kolesnichenko

Institute of Continuous Media Mechanics, RAS Ural Branch, Perm, Russia

The purification process of electrically conducting liquid consisting of non-conducting particles by electromagnetic impact was studied experimentally. We have investigated the effects of the electromagnetic force magnitude, that of the rate of transit flow and resulting secondary flows intensity and of the channel geometry on the purification efficiency. The most efficient decrease in impurity concentration occurred at a minimum value of the applied electromagnetic force due to the influence of secondary stirring flows. The maximum decrease in concentration was 87%. Based on the identified patterns, the geometry of the purification channel has been improved.

Introduction. In modern metallurgical engineering, refining of ores and liquid metals is an urgent problem of great economical significance. Refining of metals makes it possible to essentially improve their quality, namely, to increase the mechanical strength and uniformity of properties of final products. In this respect, the improvement of efficiency of ore refining and metal purification is of superior significance for metallurgists.

In industry, metals are purified by the methods of flotation, long-term sedimentation of the ore melt and by electromagnetic purification [1–3]. In the latter case, the purification of ore from waste materials occurs under the action of gravity and buoyancy due to the difference in densities of metallic and nonmetallic inclusions (oxides, sulfides and silicates). When refining large volumes of molten metal, this method appears economically unprofitable and energy-consuming, as it requires the metal to remain in a liquid state for several days.

The idea to enhance the efficiency of purification of mixture components by increasing the effective difference of the densities of carrier fluid and impurity was proposed as early as in the 1950's [4, 5]. In an electrically conducting medium, external electric and magnetic fields are capable of generating a bulk force leading to a change of the effective weight of the liquid. However, in this case, the electromagnetic force does not affect the non-conducting inclusions. Quasi-weighting of liquid metal under the action of an electromagnetic force causes the nonmetallic impurities to ascend to the surface by buoyancy [3, 5, 6]. The slag buoyed to the surface can be mechanically removed from the melt surface together with the oxide film. Despite the existence of theoretical models of electromagnetic purification, the designers had failed to invent an effective industrial device. The main problem is to choose the most appropriate design for the separating module and the most effective way of electromagnetic force application.

Physical experiments to simulate the process of electromagnetic purification of liquid metals remain a challenge. Along with high temperatures and chemical activity of working media, there are significant difficulties with introducing model impurities of a strictly specified chemical composition and proportion into the molte metal. Therefore, it seems promising to use aqueous solutions of electrolytes to simulate and study the processes of purification of non-conducting impurities in liquid metals. Thus, in [7], the possibility to control the emersion of non-conducting particles from an aqueous solution of electrolyte (sodium chloride) was shown experimentally. Due to the transparency and fluidity of electrolytic solutions at room temperature, they were found to be an appropri-

ate medium for studying MHD flows in laboratory conditions using both the optical [8, 9] and electromagnetic [10]. methods. In addition, the densities of electrolytic solutions are controlled in the process of ore beneficiation. Crushed ore is suspended in an electrolyte solution. Then the density of the solution is changed to force the non-metallic inclusions to float up to the surface. The enriched ores have a higher degree of purity and can be subjected to re-melting immediately after the purification process is finished.

Thus, it seems reasonable to perform model experiments with electrolytic solutions with the aim to investigate the refining process and the effect of initiation of secondary MHD flows under the action of superimposed electric and magnetic fields. These experiments will allow choosing an optimal method for metal purification and supply necessary data to verify numerical calculations. In contrast to the purification of liquid metals, such as Al [11, 12], modelling of the phase separation process in an electrolytic solution allows excluding the thermal problem from consideration, which greatly facilitates the modelling and establishing of basic laws.

In this work, the process of electromagnetic purification of non-conducting solid inclusions in a concentrated aqueous solution of potassium hydroxide and the effect of the resulting secondary MHD flows on the phase purification process are studied experimentally. The electromagnetic force is generated by passing an electric current through a solution exposed to an external steady magnetic field. The purpose of the study is to find the optimal channel shape and parameters of the external action, which could

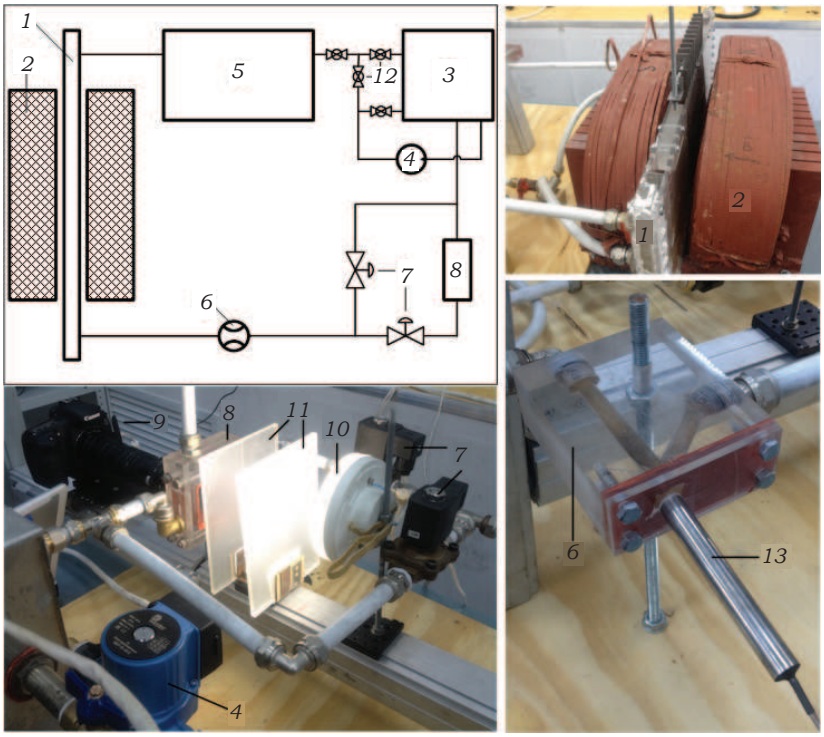

Fig. 1. The scheme of the experimental setup: *1* – purification channel, *2* – electromagnet, *3* – feed tank, *4* – circulating pump, *5* – overflow tank, *6* – flow cell, *7* – electromagnetic valves, *8* – measuring cell, *9* – camera, *10* – light source, *11* – frosted glasses, *12* – control valves, *13* – UDV probe.

ensure the greatest efficiency of the purification process. The study was carried out by considering the possibility of applying the proposed design of the purification channel when working with liquid metals.

1. Experimental setup. The experimental setup (Fig. 1) consists of a plexiglass purification channel *1* placed between the poles of an electromagnet *2*. An electrolyte solution is supplied to the channel from a feed tank *3* by a circulating pump *4* through an overflow tank *5*. After passing through the channel *2*, the electolytic solution is delivered through the pipeline to a flowmeter cell *6*, after which, depending on the position of the automatic electromagnetic valves *7*, it is pumped either into a measuring cell *8* (and then re-enters the flow tank *3*) or, bypassing the cell, immediately into the feed tank *3*. The latter flow regime allows photo tracing of the particles in the solution inside the measuring cell using a computer-controlled reflex camera *9* at rather high (more than 5 cm/s) velocities of the electrolyte flow through the system. The measuring cell is illuminated by a photodiode source *10* of light diffused through frosted glasses *11*. The flowrate of the liquid in the system is set by control valves *12* and measured by a Doppler velocimeter *13* (UDV) DOP 2000 Signal Proccesing. For correct measurement of the flowrate by UDV, a special experiment was performed to evaluate the speed of sound in an alkaline solution. Its value was 1778 m/s.

In this study, we examined the purification process in the channel (Fig. 2), which is an improved version of the purification cell in [13]. The channel was a flat rectangular cell *1*. It was furnished with a few movable partitions *2*, holding the separated impurity within the region *3*, two copper electrodes *4* for passing current through the cell, and flow equalizers *5*. The purification channel was located between the poles of the electromagnet *6*. The vertical partitions *2* were made of a material conducting an electric current. The liquid entered the channel through a nozzle *7* and flowed out through a similar nozzle *8*. The flow equalizers *5* were installed in the immediate vicinity of the edges of the electromagnet cores to prevent the formation of vortices under the influence of a non-uniform magnetic field in these zones. The electric current passing through the electrolyte interacted with an external steady magnetic field which was generated by an electromagnet consisting of a ferromagnetic core *9* and two coils *10*. The coils were con-

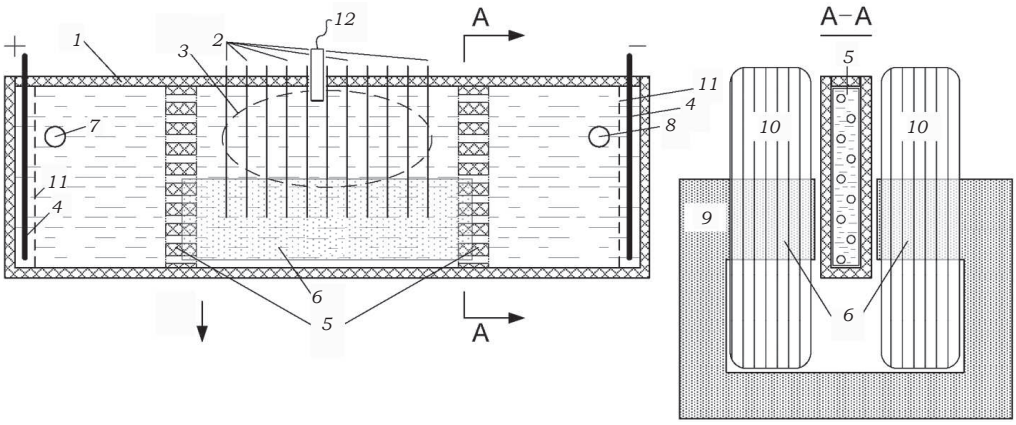

Fig. 2. Schematic of the purification channel: *1* – purification channel, *2* – movable partitions, *3* – region of action of predominantly electromagnetic forces, *4* – copper electrodes, *5* – flow equalizers, *6* – poles of the electromagnet, *7* – inlet nozzle, *8* – outlet nozzle, *9* – magnetic core, *10* – electromagnet coils, *11* - electrode grids, *12* – UDV probe.

nected in series to increase the magnitude of the magnetic field in the gap. The electric current was passed through the electrolyte in such a way as to provide quasi-weighting of the solution. Floating impurities were confined between the partitions *2* in the region *3*.

The zones of electrode location were additionally fitted with vertical grids *11* made of a non-conducting material, which were installed to trap gas bubbles generated on the electrodes during electrolysis. In the absence of such grids, a large number of bubbles can enter the separation zone and decrease its effectiveness. The secondary flows in the vertical plane of the channel were additionally controlled using a UDV *12* probe. The probe was placed vertically between two retention partitions *2*. The UDV probe was used to estimate the velocity of secondary vortices in the separation channel. It is important because the interaction of the external magnetic field and the electric current leads to the generation of vortex flows in the liquid in the zones of non-uniform current [14].

The electromagnet was fed by the DC current from the HEIDEN power HP 15100. The current passing through the electrolyte was supplied from the MASTECH DC Power Supply HY 3005-2. An aqueous solution of potassium alkali was used as the working fluid. The impurities were carbon particles with sizes ranging 10 to 300 μm.

Prior to experiments, we estimated the intensity of the magnetic field in the gap of the electromagnet as a function of the coil current value. Magnetic induction measurements were made using the Lake Shore 421 Gaussmeter. The resulting dependence is linear.

The concentration in the alkaline solution was determined by its density using a hydrometer. The density of the medium (taking into account the impurity of carbon particles) was $1.144 \pm 0.001\,\mathrm{g/cm^3}$. The alkali concentration was $\mathrm{C} \sim 16\%$. Due to the slightly different densities of the solution and the impurity particles, the model particles are not suspended in the solution and deposit onto the bottom under gravity. It is explained by the non-uniform size distribution of the particles. The mean particle density was 1.20–$1.25\,\mathrm{g/cm^3}$. In order to prevent complete sedimentation of the impurity particles, the solution in the feed and overflow tanks was mechanically stirred by the blades rotated by electrical drives.

2. Measurement technique. The relative concentration of impurity particles was measured in a measuring cell using a Cannon EOS 60D camera. The cell was a U-shaped frame made of plexiglass. The front and rear walls of the cell, positioned parallel to each other, were made of silica glass. The lower part of the measuring cell was fitted with inlet and outlet pipes to provide a continuous flow of the alkaline solution. The upper surface of the alkaline solution in the cell was free, allowing removal of gas bubbles which are formed during the electrolysis and carried into the measuring cell by the flowing solution. The alkali layer in the cell was illuminated by a LED lamp. The light passed through three frosted glasses to ensure uniform illumination and to avoid light-striking of the areas around the LEDs. The thickness of the alkali layer in the cell was 10 mm. The depth of the sharply imaged zone was 2 mm. During the experiments, appropriate image focusing was achieved by presetting the focus control lens of the camera in the middle position between two glasses. It means that the medial region of the measuring cell, corresponding to the most intense flow, was considered. Due to the low velocity of the flowing solution (10–15 mm/s), the displacement of the impurity particles per one subsequent frame was insufficient to cause noticeable diminution of the image quality. The shooting frequency was 2 frames per minute, whereas the total duration of shooting was 90 minutes. The resulting images were digitally processed to determine a relative concentration of the impurities. During each measurement, the illumination degree was kept constant due to the light isolation of the room.

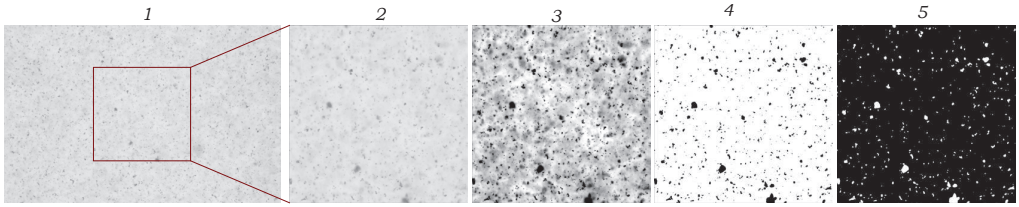

Fig. 3. An example of images processing for concentration measurement: *1* – original photo, *2* – grayscale image, *3* – grayscale image, *4* – binarized image, *5* – inverted binarized image.

Images were processed in MATLAB. First, a square area was cut out of the photo with the aim that further processing should be done just for this segment (Fig. 3). This made it possible to exclude the influence of the boundaries of the imaged region on the degree of illumination and concentration in the stagnant zones of the measuring cell. The resulting full-color RGB image was converted into a two-dimensional grayscale array. Conversion to grayscale images was made in two steps. At the first stage, a full-color image was converted to a grayscale image with the gamma correction coefficient equal to unity by considering the specified image intensity of the original image which was evaluated based on the minimum and maximum image brightness. At the second stage, the resulting image was made grayscale again using gamma correction. The initial and the final degree of the image intensity ranged from zero to unity. To increase the contrast ratio of the grayscale image, it was dimmed using gamma correction with $\gamma = 1.5$. Then, the cutoff level was selected empirically during the conversion of a grayscale image to a binary (black and white) one. The criterion for selection was the requirement that one could distinguish the finest fraction of impurities while keeping the image intensity high enough to detect the localization of individual particles. To suppress digital noise in a binary image, we used the method of median filtering for nine adjacent pixels in each direction.

After image processing, two versions of optic analysis were used. In the first case, the total amount of impurity (unit values corresponding to the presence of particles) was calculated against a zero background. It means that the concentration of particles was found from the relative degree of image darkening as the ratio of the number of white (with a value of one) pixels to the total number of pixels (the total size of the processed image area). Let us name this method optical measurements. In the second

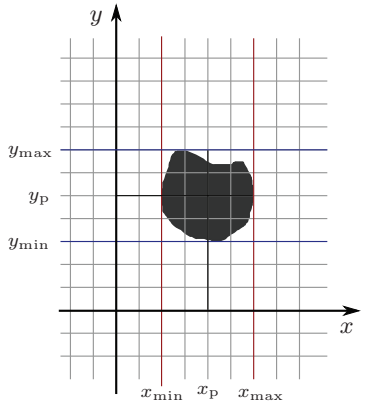

Fig. 4. Schematic representation of the method of localization of individual impurity particles.

case, a fractional analysis of the concentration variation was made. In this case, standard software tools were used to find the location of individual impurity particles in a binary image and to calculate their size and position. The position of the particles $\{x_\mathrm{p}, y_\mathrm{p}\}$ on the coordinate axes was determined as the mean value between the maximum and minimum coordinates of the area occupied by a particle on the corresponding axis (Fig. 4) according to Eq. (2). The effective particle size r_p was estimated as the radius of a circle, the area of which is similar to that of the particle considered. The data obtained were grouped according to the predetermined particle size ranges. Therefore, particles with the effective radius of less than 1.30 μm and more than 260 μm were not considered. To plot the final concentration curve, the concentration values of the individual fractions were added with the corresponding weights equal to the average particle radius. Hereinafter, we will name this method fractional analysis:

$$x_\mathrm{p} = \frac{x_\mathrm{max} + x_\mathrm{min}}{2}, \quad y_\mathrm{p} = \frac{y_\mathrm{max} + y_\mathrm{min}}{2}. \tag{1}$$

Fig. 3 illustrates the stages of photo processing. Processing of a series of photos made it possible to obtain the dependence of the relative concentration of impurity particles on the time in the ratios of the area occupied by the particles in the photo to the total area of the photo. An graph plotted for the case of gravitational sedimentation of particles is presented in Fig. 5.

The difference of the final concentration curves is due to a predominant contribution of the fine fractions, which rapidly rises to the surface under the influence of electromagnetic forces already at the initial stage. The threshold of optical binarization cutoff in the optical method is assumed slightly higher than in fractional analysis, which explains why curve *1* gives an underestimated value of the concentration, as opposed to curve *2*. This was set to exclude digital noise when analyzing the degree of image darkening because the smallest fraction and particles, which do not fall within the zone of a sharp image, produce general background darkening. A further decrease of the concentration detected by the optical method is due to the purification of a large fraction, namely, the fraction of larger particles, which is excluded from fractional analysis. In optical analysis, the largest particles significantly contribute to image darkening, so curve1 descends much faster than curve *2*.

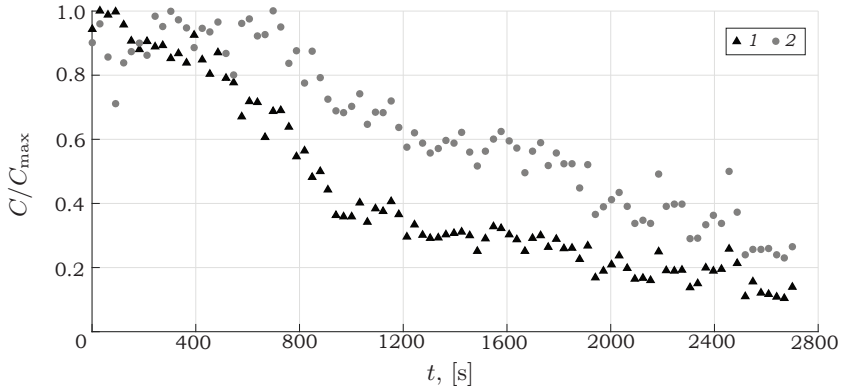

Fig. 5. Variation of the impurity concentration in alkali solution for the case of gravitational sedimentation obtained by two methods: *1* – direct optical measurements, *2* – fractional analysis.

As numerical estimates of the method's errors, the relative influence of the gamma correction on the obtained concentration curves at 6% and the relative influence of the binarization cutoff at 13% can be taken. Both errors were found for the processing parameters changing in the range of values from 50% to 200% relative to the operating values.

3. Results. During the study, we investigated the efficiency of impurity separation depending on the electromagnetic force magnitude, on the transit flow velocity in the purification channel, on the retention partition, on the conditions at the electrolyte upper surface, and on the channel inclination angle in relation to the direction of gravity.

Since the degree of electrolyte weighting depends on the magnitude of the electromagnetic force, one can expect that with an increase of the magnetic field intensity the weight difference between the impurity particles and the liquid will also increase, which contributes to the purification efficiency. However, the excitation of an electromagnetic force can give rise to vortex flows which develop in the electrolyte due to the presence of multiple non-uniformities in the electric current due to the channel design. The intensity of such vortex flow increases with an increase of the applied force. This leads to stirring of the medium and enhances the efficiency of the purification process. Therefore, it is necessary to find a regime which provides a balance between the mechanisms of quasi-weighting of the liquid and the generation of stirring flows. The intensity of the electromagnetic action was controlled by changing the magnetic field induction, because varying the strength of the electric current passing through the electrolytic solution causes an electrochemical reaction. Electrolysis, which proceeded in the zone with electrodes at high values of the current strength, led to the formation of numerous gas bubbles which weakened the electrical contact with the electrolyte solution. In addition, part of the impurity particles was carried away by the bubbles during flotation and created an additional undesirable mechanism which decreases the concentration of impurity particles. On the other hand, the passage of low-strength electric currents through the electrolyte also causes certain difficulties associated with the occurrence of electrochemical processes on the surface of the current circuits, which creates a potentials difference at this interface. Thus, all measurements were made for an electric current of 1.7 A. With this current value, it becomes possible to decrease the effect of the chemical processes on the electrical properties of the system and, at the same time, to avoid intense gas release.

Fig. 6 shows concentration curves versus time at different values of the applied external magnetic field. It is seen that the best result is obtained at a minimum magnitude

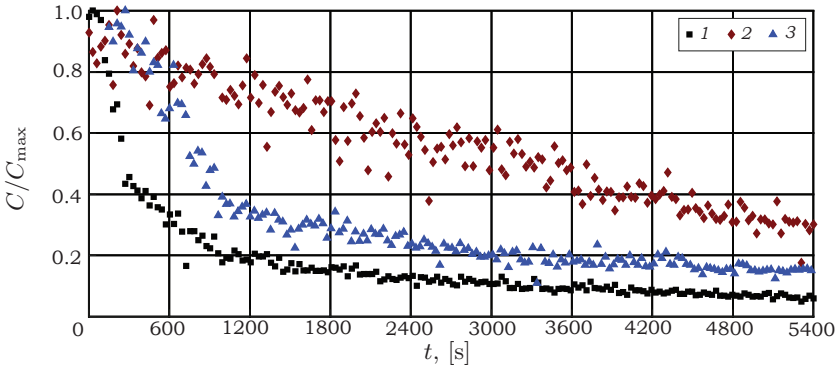

Fig. 6. Concentration variation of carbon particles in alkali solution during their purification at different values of the external magnetic field B: *1* – 0.235 T, *2* – 0.465 T, *3* – 0.695 T.

of the applied magnetic field (0.235 T). In this case, the vertical velocity measured by the UDV probe was approximately 7 mm/s. Under the action of the magnetic field of higher strength ($B = 0.695$ T), the vertical velocity component experienced significant fluctuations in the range of 5–10 mm/s. In the intermediate case, when the magnetic field was induced at $B = 0.465$ T, a decrease of the impurity concentration occurred by a law which is close to a linear one (compared to the exponential decrease in the previous cases). The vertical component of the velocity was in the range of 10–12 mm/s. Thus, the hypothesis about the negative influence of secondary flows on the purification process has been substantiated.

The purification efficiency is governed by the transit flow velocity (and, hence, by the flowrate), since in industrial applications it is more convenient to purify molten metals during transfer rather than during pumping in a closed loop (an exception is the cooling loop of the fast neutron reactor when it is necessary to periodically remove oxides from the coolant). Fig. 7 shows concentration curves for different flowrates. With increasing transit flowrate, the residence time of the polluted medium in the zone of electromagnetic purification decreases and, as a result, the purification efficiency decreses. In addition, a fast transit flow leads to concentration fluctuations due to the sedimentation of impurities on the retention partitions and removal of the deposited particles by an overtaking flow. The flow generated between the partitions has a two-vortex pattern. The size and intensity of the vortex vary with time. The average flowrate is approximately 8 mm/s for the flowrates $Q = 10.4 \cdot 10^{-6}$ and $Q = 14.9 \cdot 10^{-6}$ m^3/s and is approximately 11 mm/s for the flowrates $Q = 5.88 \cdot 10^{-6}$ m^3/s. A small difference in the velocities of the secondary flows indicates that the residence time of the liquid in the separation region has a greater impact on the purification efficiency than the intensity of the secondary flows.

Changing the position of the retention partitions affects the total surface area with the impurities. By raising a partition or removing it from the channel, one can decrease the hydraulic resistance to the electrolyte flow and change the flow velocity in the field of electromagnetic force. Fig. 8 displays concentration curves for three positions of the retention partitions. An immersion depth of 132 mm corresponds to the complete immersion of the partitions in the channel (note that the partitions create the greatest resistance to the flow), an immersion depth of 68 mm implies that the lower edges of the

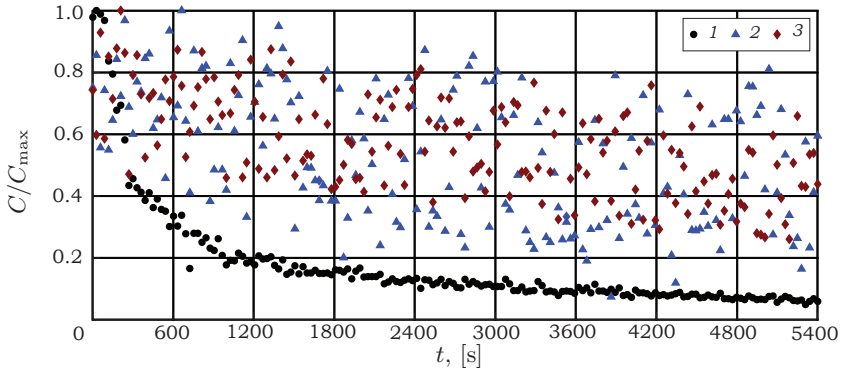

Fig. 7. Relative variations in the concentration of carbon particles in alkali solution during their separation at different flowrates Q in the fluid pumping system: *1* – $Q = 5.88 \cdot 10^{-6}$ m^3/s, *2* – $Q = 10.4 \cdot 10^{-6}$ m^3/s, *3* – $Q = 14.9 \cdot 10^{-6}$ m^3/s.

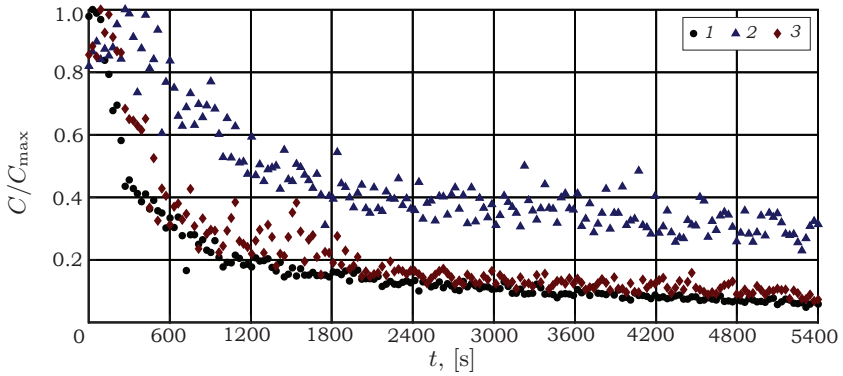

Fig. 8. Relative variations in the concentration of carbon particles in alkali solution during their separation at different positions of the partitions in the purification channel relative to its upper boundary: *1* – 132 mm, *2* – 100 mm, *3* – 68 mm.

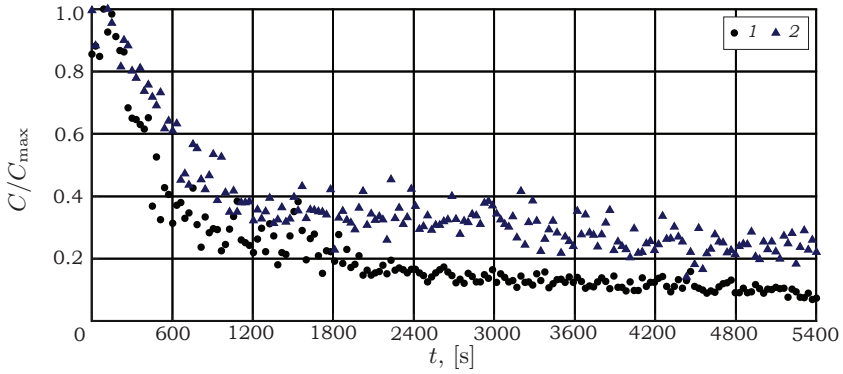

Fig. 9. Relative variations in the concentration of carbon particles in alkali solution during their separation at different positions of the partitions in the purification channel relative to its upper boundary: *1* – 132 mm, *2* – 100 mm, *3* – 68 mm.

partitions are in contact with the free surface of the electrolyte (i.e. the partitions do not impede the flow). In the intermediate position, the partitions only partially impede the fluid flow. The figure shows that the purification efficiency remains unchanged for the completely immersed and completely lifted partitions. At the same time, the partially raised partitions decrease the efficiency of purification almost twice. This is explained by the formation of more intense vortex patterns in the channel which stir the liquid and entrain the impurity particles deposited on the partitions. The velocity of such secondary flows reaches 20 mm/s and exceeds the velocity of the flow through the channel.

One of the important problems of the purification process is where and how the impurity removed from the main flow is held. In order to determine the contribution of the surface tension forces at the liquid upper surface, additional experiments were carried out with a top solid cover. The cover was made of alkali-resistant rubber and installed horizontally in the channel, the retention partitions and the UDV probe were completely removed from the channel. Concentration curves for two configurations of the top surface of the liquid are plotted in Fig. 9. The difference in the final concentration is relatively small, which suggests that the effect of the surface tension forces of the electrolyte on the refining process is not substantial. Nevertheless, the final concentration value in the

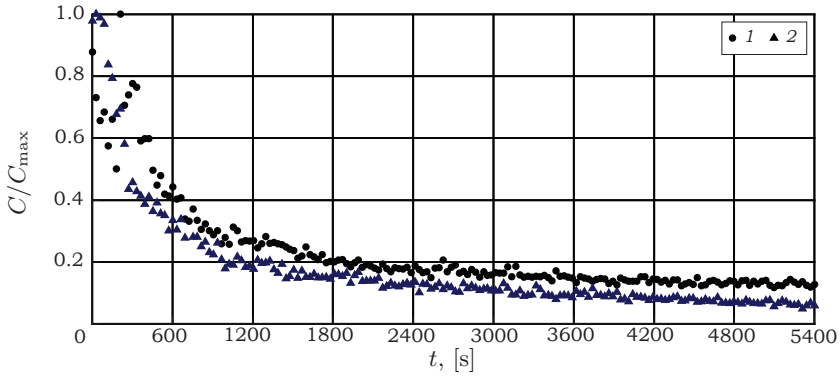

Fig. 10. Relative variations of the concentration of carbon particles in alkali solution during their separation at different angles of inclination of the purification channel to the direction of gravity: *1* – $\alpha = 0°$, *2* – $\alpha = 4.6°$.

experiment with the free surface indicates that part of the impurity particles is held by the surface tension forces.

The pattern of the secondary flows between the retention partitions is similar to that of a convective plume. As a result, the inclination of the channel to the direction of gravity can change the pattern of the secondary flow (a roller elongated along the vertical axis of the channel). The channel can be inclined due to the flexibility of the metal-plastic connecting tubes. The inclination angle is defined using a digital level gauge. A channel tilt of approximately 4.6° produced a weak effect on the purification efficiency, it only slightly enhanced it (Fig. 10). The measurements by the UDV probe showed that the flow initiated in the inclined channel was actually a large-scale circulation, involving an additional vortex of greater intensity in the region of the transit flow.

Conclusion. The process of electrolytic solution refining from non-conducting impurities was investigated experimentally. We have studied the effect of the applied electromagnetic force magnitude and intensity of the resulting secondary flows on the efficiency of the purification process. It has been found that the greatest decrease in impurity concentration occurs at a minimum value of the applied electromagnetic force. This effect could be explained by the occurrence of secondary stirring flows which prevent the retention of impurities in the purification channel. The maximum decrease in concentration was 1/8 of the initial value.

The obtained dependence of the purification efficiency on the flowrate of the transit flow shows that the lower is the velocity of the flow, the more effective is the applied purification method. At flowrates of more than $6{\cdot}10^{-6}\,\mathrm{m}^3/\mathrm{s}$, the actual residence time of the liquid in the zone of electromagnetic action is insufficient for a proper phase separation. The removal of the retention partitions does not significantly affect the purification process. At the same time, the partitions, when partially removed from the separation zone, create conditions for the formation of secondary stirring flows of high intensity. Therefore, when designing electromagnetic separators, it seem reasonable to exclude partitions from the channel design, which essentially simplifies its shape. The latter is critical for ensuring the safety of structures interacting with liquid metals. Placing of a solid top cover over the channel does not significantly affect the purification process, however, this can reduce its efficiency by 30%. Therefore, liquid metal refining can be realized in closed channels which have no contact with the atmosphere. This will not only decrease

the atmospheric contamination with metal vapors during the operation of the refining chamber, but protects the metal from oxidation by atmospheric oxygen. The inclination of the purification channel with respect to the direction of the gravitational force allows controlling the secondary flows. Thus, it is possible to intensify the transfer of impurities from the region of the transit flow of liquid metal to the stagnant zones of the purification channel.

References

[1] S. Makarov, R. Ludwig, and D. Apelian. Inclusion removal in molten aluminum: Mechanical, electromagnetic, and acoustic techniques. *Trans. Am. Foundrymens Soc.*, vol. 107 (1999), pp. 727–735.

[2] S. Makarov, R. Ludwig, and D. Apelian. Electromagnetic separation techniques in metal casting. I. Conventional methods. *IEEE Transactions on Magnetics*, vol. 36 (2000), no. 4, pp. 2015–2021.

[3] Z. Xu, T. Li, and Y. Zhou. Continuous removal of nonmetallic inclusions from aluminum melts by means of stationary electromagnetic field and dc current. *Metallurgical and Materials Transactions A*, vol. 38 (2007), no. 5, pp. 1104–1110.

[4] D. Leenov and A. Kolin. Theory of electromagnetophoresis. I. Magnetohydrodynamic forces experienced by spherical and symmetrically oriented cylindrical particles. *The Journal of Chemical Physics*, vol. 22 (1954), no. 4, pp. 683–688.

[5] I.L. Povh, A.B. Kapusta, B.V. Chekin *Magnetohydrodynamics in metallurgy (In Russian)* (1974).

[6] L. Zhang, *et al.* Application of electromagnetic (EM) separation technology to metal refining processes: A review. *Metallurgical and Materials Transactions B*, vol. 45 (2014), no. 6, pp. 2153–2185.

[7] J.P. Park, Y. Tanaka, K. Sassa, and Sh. Asai. Elimination of tramp elements in molten metal using electromagnetic force. *Magnetohydrodynamics*, vol. 32 (1996), no. 2, pp. 227 – 234.

[8] J. Takeuchi, *et al.* Experimental study of MHD effects on turbulent flow of Flibe simulant fluid in circular pipe. *Fusion Engineering and Design*, vol. 83 (2008), no. 7–9, pp. 1082–1086.

[9] M.R. Afshar, M.R. Aboutalebi, R. Guthrie, and M. Isac. Modeling of electromagnetic separation of inclusions from molten metals. *International Journal of Mechanical Sciences*, vol. 52 (2010), no. 9, pp. 1107–1114.

[10] O. Andreev, C. Haberstroh, and A. Thess. Mhd flow in electrolytes at high hartmann numbers. *Magnetohydrodynamics*, vol. 37 (2001), no. 1–2, pp. 151–160; DOI: http://doi.org/10.22364/mhd.37.1–2.19

[11] E.-P. Yoon, *et al.* Continuous elimination of Al_2O_3 particles in molten aluminium using electromagnetic force. *Materials Science and Technology*, vol. 18 (2002), no. 9, pp. 1027–1035.

[12] L. Zhang and L. Damoah. Current technologies for the removal of iron from aluminum alloys. *TMS Light Metals*, (2011), pp. 757–762.

[13] G. Losev, A. Mamykin, I. Kolesnichenko. Electromagnetic separation: concentration measurements. *Magnetohydrodynamics*, vol. 55 (2019), no. 1–2, pp. 89–96; DOI: http://doi.org/10.22364/mhd.55.1–2.11

[14] D. Shu, *et al.* Effects of secondary flow on the electromagnetic separation of inclusions from aluminum melt in a square channel by a solenoid. *ISIJ International*, vol. 42 (2002), no. 11, pp. 1241–1250.

Received 15.01.2021